

H. Basic Studies of Ultrasonic Welding for Advanced Transportation Systems

Principal Investigator: Zhili Feng

Oak Ridge National Laboratory

1 Bethel Valley Road, Oak Ridge, TN 37831

(865) 576-3797; fax: (865) 574-4928; e-mail: fengz@ornl.gov

Technology Development Area Specialist: Sidney Diamond

(202) 586-8032; fax: (202) 586-1600; e-mail: sid.diamond@ee.doe.gov

Field Technical Manager: Philip S. Sklad

(865) 574-5069; fax: (865) 576-4963; e-mail: skladps@ornl.gov

Participants:

Michael L. Santella, Oak Ridge National Laboratory

Edward A. Kenik, Oak Ridge National Laboratory

Xiaoguang Zhang, Oak Ridge National Laboratory

Hsin Wang, Oak Ridge National Laboratory

Keyu Li, Oakland University

Contractor: Oak Ridge National Laboratory

Contract No.: DE-AC05-00OR22725

Objective

- Develop a fundamental understanding of the ultrasonic welding (UW) process.
- Establish process conditions to optimize joint properties of aluminum alloys for auto body applications.
- Explore opportunities for joining dissimilar materials.
- Explore the feasibility of ultrasonic processing in other novel and unique situations in materials processing, such as making powders more dense, producing functionally graded components, modifying surface properties, and producing dissimilar material joints.

Approach

- Perform UW experiments to develop correlations of process parameters with joint properties.
- Characterize details of joint microstructures.
- Model the fundamental interactions of ultrasonic waves with solids.

Accomplishments

- Related the microscopic features at the interface region to process conditions.
- Initiated a study toward the geometric effects on ultrasonic energy generation and dissipation during the welding process.
- Completed a preliminary study of acoustic energy distribution by means of infrared thermography.
- Initiated an experimental study of residual stress distribution in the bonding region.

Future Direction

- Continue welding process development for dissimilar materials, including joining of amorphous metals.
- Study the structure-property relationship of joints.
- Model the acoustic energy distribution in the weld joint.
- Study the residual stress distribution in the bonding region.
- Assess the ability of ultrasonic processing to enhance the densification of powder metal compacts.

Introduction

UW uses high frequency mechanical vibrations to produce a solid-state metallurgical bond (weld) between metals. The basic process setup is illustrated in Figure 1 for a typical spot weld configuration. An electro-mechanical converter converts high-frequency electric current to mechanical vibrations. The mechanical vibration is then modulated and amplified by the booster/horn before it is applied to the overlapping workpiece through the sonotrode. A moderate clamping force is applied to ensure the mechanical vibration is transferred to the sheet-to-sheet interface (the faying surface) where the weld is created. Typically, the mechanical vibration is at 20–40 kHz with an amplitude range of 5–50 μm. The power delivered to the workpiece is in the range of several hundred to several thousand watts.

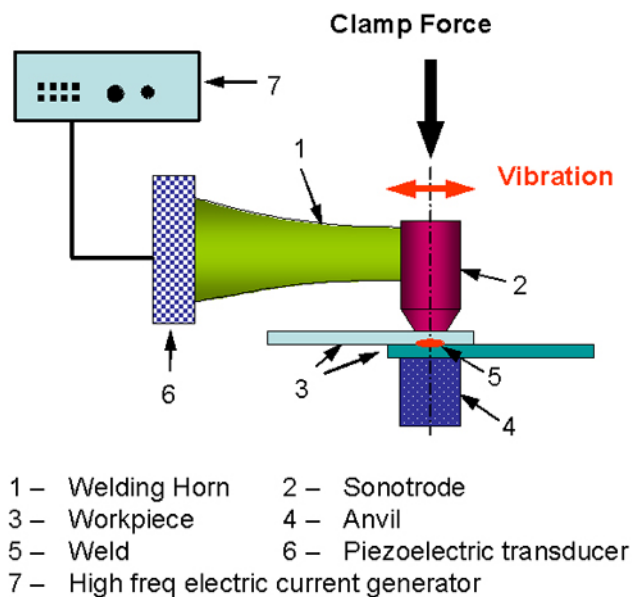


Figure 1. Schematic setup of ultrasonic welding process.

The principles for the formation of the metallurgical bond are illustrated in Figure 2. The combination of clamp pressure and mechanical vibration produces several important effects in the formation of the metallurgical bond at the workpiece interface. The lateral mechanical vibration of the sonotrode causes a small amount of relative motion at the interface between the two workpieces. The frictional action at the interface due to the relative motion and the pressure breaks the surface oxides and other contaminants. As a result, clean metal surfaces are brought into contact under pressure. Frictional heating also occurs at the bond interface. The heating promotes both localized deformation and diffusion in the region where the pressure is applied. When the process conditions are right, metallurgical bonds can be obtained without melting at the bonding interface. The self-cleaning nature of UW and its ability to form metallurgical bonds without melting are both important advantages of the process.

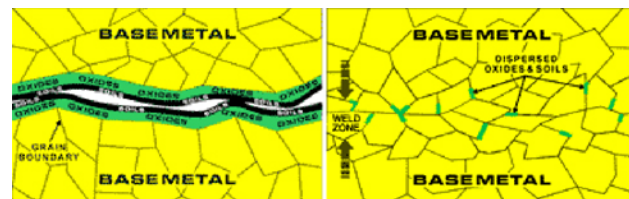


Figure 2. Schematic representation of bond interface before (left) and after (right) UW.

UW creates a joint without bulk melting. Thus the ultrasonic weld is inherently immune to welding defects associated with the solidification process in fusion welding. These include solidification cracking and porosity due to absorption of gaseous impurities (N, H, O) by the liquid metal that are common in electrical resistance spot welding (RSW) (the most widely used joining process in auto body assembly) of many classes of materials used in auto-

motive body structures. Also, unlike the copper-based electrode used in RSW, the sonotrode in UW can be made of high-strength materials that are inert to chemical attack from the material to be welded. Therefore, UW offers several significant potential advantages in joining aluminum alloys and other high-performance lightweight materials for auto body structures.

This program started in FY 2003. The FY 2003 study demonstrated the feasibility of UW of aluminum alloys, magnesium alloys, and steel to themselves, and the feasibility of joining dissimilar metals (aluminum alloy to steel). The FY 2004 efforts included microstructural characterization at the bonding interface, study of ultrasonic energy distribution in the weldment, and exploratory investigation of welding residual stresses. We also initiated the development of theoretical models that would eventually allow for interrogation of geometry effects on the distribution of acoustic energy, an important issue for application of the UW process. The variation of weld strength as a function of time was also observed.

Welding

All welding trials were conducted on a Sonobond ultrasonic welder. The machine operated at 20 kHz and had a maximum rated power output of 2500 W.

All welds were made using 25-mm-wide and 100-mm-long specimens. This is a standard coupon dimension commonly used by the auto industry for weldability testing of resistance spot welds. All specimens had a nominal thickness of 1 mm. For bonding interface microstructural characterization, a standard 1-in overlapping configuration shown in Figure 3 was used. The weld was made at the center

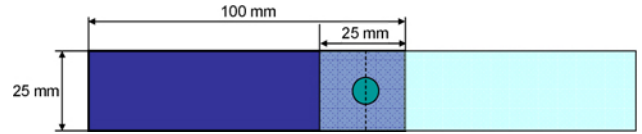


Figure 3. Weld coupon dimensions used in the study.

of the overlapping region. For study of the geometry effects, the amount of overlap and the location of the weld were systematically varied.

Microstructure Characterization

Because of the solid-state nature and minimal thermomechanical excursion of the ultrasonic bonding process, the bonding interface between the same metal (for example, Al6061 to Al6061) was difficult to observe experimentally. To aid the bonding interface study, a series of dissimilar welds between two different aluminum alloys (Al6061-T4 and Al2024-T3) were used. These two aluminum alloys have very different etching responses to Keller’s reagent. This allowed for selective etching to reveal the interface region of the weld.

The nominal mechanical properties of the two aluminum alloys are summarized in Table 1. As shown in the table, Al6061 is always softer and has better ductility than Al2024 over the entire temperature range. The differences in the mechanical properties of the two alloys are considerable at the ambient temperature, but they diminish as the temperature increases. At 370°C, the tensile strength and ductility of the two alloys are very close to each other. The differences in mechanical properties are considered to be an important factor affecting the interfacial deformation and bonding behavior during welding.

Table 1. Mechanical properties of Al6061-T4 and Al2024-T3 at selected temperatures
(Source: *Properties of Aluminum Alloys*, AMS International, 1999)

	25°C			260°C			370°C		
	Yield (MPa)	Tensile (MPa)	Elong g (%)	Yield (MPa)	Tensile (MPa)	Elong g (%)	Yield (MPa)	Tensile (MPa)	Elong (%)
6061-T4	145	241	25	165	172	17	55	59	35
2024-T3	345	483	17	241	269	17	69	76	35

We have discussed some of the general microstructural characteristics in the bonding interface region as a function of welding process parameters in the FY 2003 annual report. Additional observations are reported here. All the cross-sectional photos were taken along the plane cut through weld center, as depicted by the dashed line in Figure 3.

Figure 4 shows the bonding interface at two different energy levels. The pictures were taken near the center of the weld (labeled A in Figure 5). At low energy levels, the bonding interface is quite flat microscopically. The interface becomes wavy, and considerable microscopic swirling deformation is evident at high energy levels. The microscopic swirling deformation is confined primarily on the softer Al6061 material side.

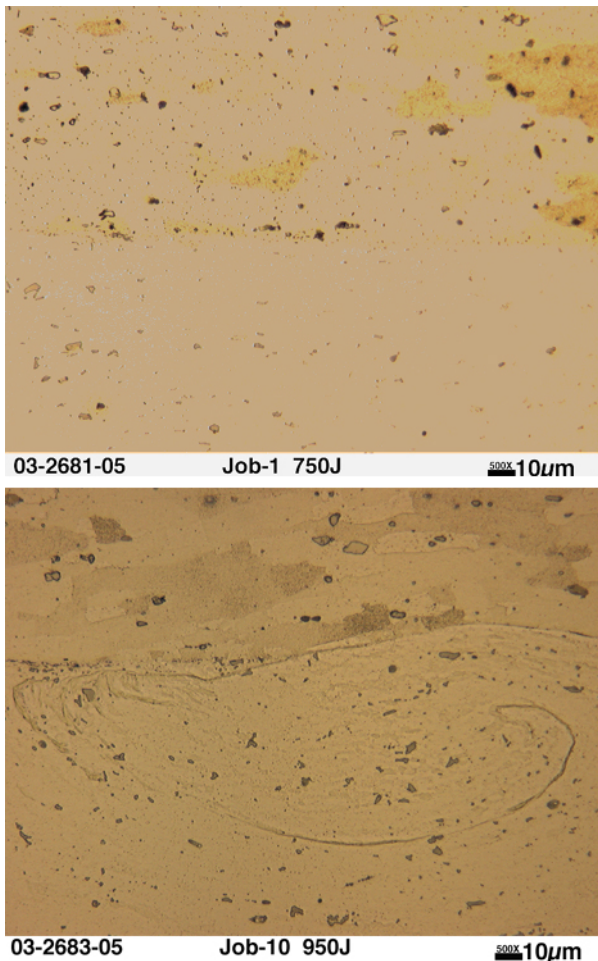


Figure 4. Changes in bonding interface flatness as a function of UW energy level. Top: 750J; bottom: 950J. Other process conditions: 2400 W and 70 psi. Al2024 is the upper sheet.

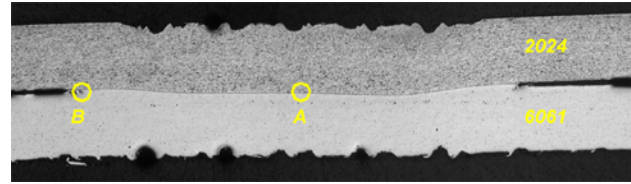


Figure 5. Macro view of the weld cross-section. The observation positions in Figure 4 and Figure 6 are labeled A and B, respectively. Point A is near the center of the weld; Point B is at the edge of the bonded region.

Figure 6 shows the deformation near the periphery (region B in Figure 5) of the bonded interface in the low-energy-level case (750J). It was taken from the same 750J weld as the top photo of Figure 4. It suggested that, even though the interface was relatively flat when the energy level was low, the microscopic deformation was still extremely large and mainly confined on the softer Al6061 side.

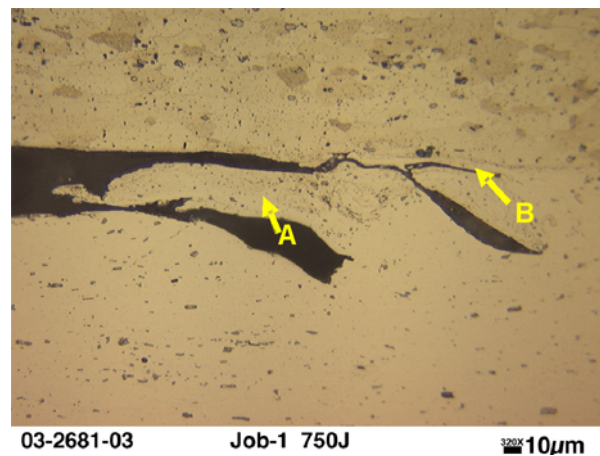


Figure 6. Local deformation of Al6061 at the periphery of the bonding interface. The photo was taken at position B of Figure 5. Arrow B points to the region where “coating” is formed. Energy level: 750 J.

These observations suggest that there is considerable shearing deformation at the interface, under the lateral rubbing motion of the sonotrode, under all energy levels studied in this program. On the other hand, the material deformation or motion vertical to the interface is secondary to the bonding process and only becomes noticeable when the ultrasonic energy level is high.

Another intriguing observation is the “coating” phenomenon at the interface. As pointed to by arrow B in Figure 6, a thin layer of Al6061 is “coated” and bonded onto the Al2024 side, while this thin layer is

still disconnected with the bulk of the Al6061 material. This phenomenon is more evident in Figure 7, where only intermittent, partial bonding is achieved at the interface at a very low energy level (550J).

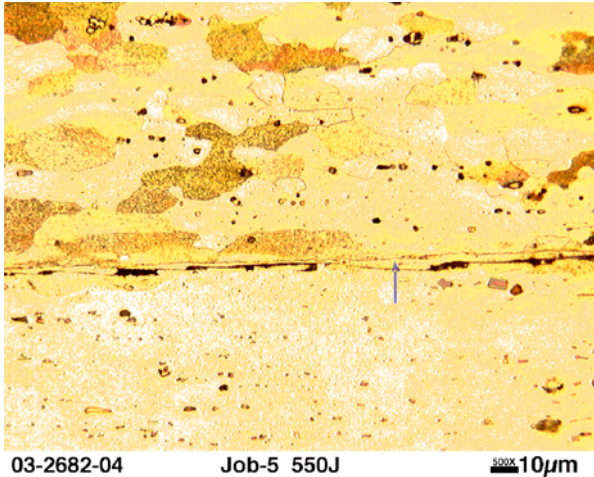


Figure 7. Coating of Al6061 to Al2024 at a low energy level (550 J) that could form only partial bonding.

Although the causes for formation of the coating layer are not clear at this time, the fact that it forms in the early stage of the bonding process would be an important aspect of the bonding process during UW.

At higher energy levels, the bonding interface becomes wavy and is generally considered to be beneficial to the joint strength of the ultrasonic welds. However, excessive energy could cause cracking of the material, as shown in Figure 8. For the Al6061-to-Al2024 welds, the cracking always occurs on the Al2024 side, more or less parallel to the bonding interface at a distance about 50 to 100 µm from the interface. One possible cause would be related to the lower ductility of Al2024 between the room-to-intermediate-temperature range as shown in Table 1.

Geometric Effects on the Ultrasonic Bonding Process

We observed strong geometric dependence of the process: the weld quality, energy input, and energy distribution are all strongly dependent on the geometric arrangements of the test. Such dependency needs to be thoroughly understood because of

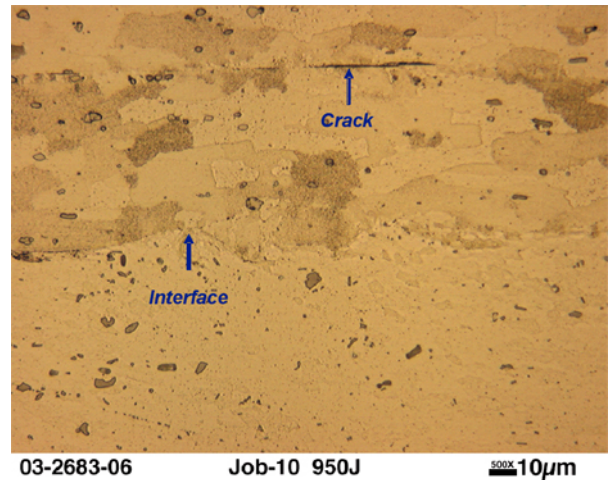


Figure 8. Cracking at Al2024 side of bonding interface due to excessive energy input.

its important implications in the industrial applications of the process.

Effects of vibration direction relative to weld coupon orientation. Figure 9 compares two welds made when the direction of the applied lateral mechanical vibration from the sonotrode was changed relative to the specimen orientation. The direction of vibration is depicted by the arrow next to the weld in the figure. All other welding conditions were identical when these two welds were made. When the vibration was in the width direction of the specimen, two cracks formed at the edge of the specimen, as shown in the lower part of Figure 9. Such cracking was absent when the vibration was applied along the length direction of the specimen. This suggests that the acoustic energy distribution in the weld coupon (or welded structure) is strongly dependent on the vibration direction relative to the geometric orientation of the part.

It is also important to note that, although the two cracks are relatively symmetric to the weld, they are not connected to the weld. This indicates that the cracks are not originated by the directly applied vibration of the sonotrode. Rather, there must be high energy concentration points (hot spots) near the edge of the plate, caused by the complex interaction of the propagating acoustic wave from the excitation source and the reflected wave from the free boundaries of the specimen.

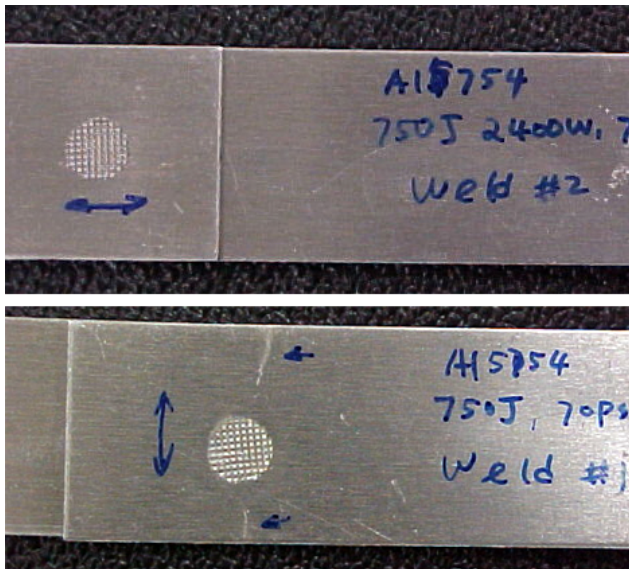


Figure 9. Effect of vibration direction for Al5754. 750 J, 2400 W, 70 psi. Top: vibration parallel to specimen length. Bottom: vibration parallel to specimen width.

Clearly, proper control and elimination of undesired hot spots would be a critical issue for the application of UW.

Interactions of multiple welds. Auto body structures generally require multiple spot welds to connect two structural members. On average, about 3000 to 5000 spot welds are used in assembling a passenger vehicle. In this study, the three-weld test arrangement commonly used in RSW was used to investigate the interactions between the adjacent ultrasonic welds, and the results are intriguing.

Figure 10 shows the three-weld arrangement used in the study. The two 25 × 100 mm Al5754 coupons were overlapped by approximately 75 mm in the length direction. The three welds were made one after another, following the sequence labeled in the figure. The first weld was placed at the center of the 75-mm overlap (i.e., 37.5 mm from the edge of the plate). The second and third weld were made respectively to the left and the right of the first weld, at a nominal distance of 20 mm from the first weld. The welds were produced with identical settings: 2400 W, 70 psi, and 0.35 s. The vibration from the sonotrode was along the width direction of the specimen as illustrated in the figure.

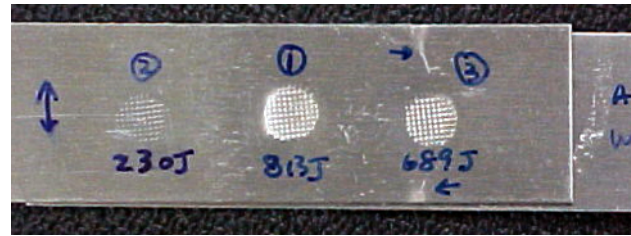


Figure 10. Interactions of multiple welds on the energy input level. All three welds were made with the same welding parameters: 2400 W, 70 psi, and a welding time set at 0.35 s. Weld ID = 4. Material: Al5754.

The energy output as recorded by the ultrasonic machine was drastically different. The system delivered 813 J of energy when making the first weld, quite close to the theoretical value of 840 J (100% energy efficiency) under perfect acoustic impedance matching. However, because of the constraint changes induced by the first weld (as well as the location effect of the second weld), the energy output when making the second weld was only 230 J, less than 1/3 of the energy output in making the first weld. In this particular case, metallurgical bonding was not achieved in the second weld because of the inadequate energy input. The energy output in making third weld was 689 J. Note again the cracks near the third weld that were produced in making the third weld.

The multiple-weld study clearly shows that the acoustic impedance of the UW system can be greatly affected by prior welds made during the assembly process. This would have profound influence on the energy output level and could cause considerable weld-to-weld quality variations.

Infrared Thermography Study of the UW Process

The welding trials clearly show that the distribution of the acoustic energy in a UW workpiece is very complicated and has a profound influence on the weld quality. To further understand this matter, a study was initiated in FY 2004 in which real-time infrared (IR) thermography was used to capture the temperature changes during the UW process. Both the spatial distribution and the temporal variation of the temperature field were used to infer how the heat (the dissipative part of the acoustic energy) is generated and distributed during UW.

The real-time IR measurements were conducted using a high-speed, high-sensitivity (0.015 K) and high-spatial-resolution (5 $\mu\text{m}/\text{pixel}$) IR camera. In the first test, the energy distribution across the workpiece thickness was captured with a special experimental set-up, as shown in Figure 11. The welds were made at the edge of the two workpieces, and the sonotrode vibration was parallel to the long side of the specimen. This special experimental setup preserved the process symmetry in an actual welding situation, while allowing the weld cross-section to be exposed to the IR camera during welding.

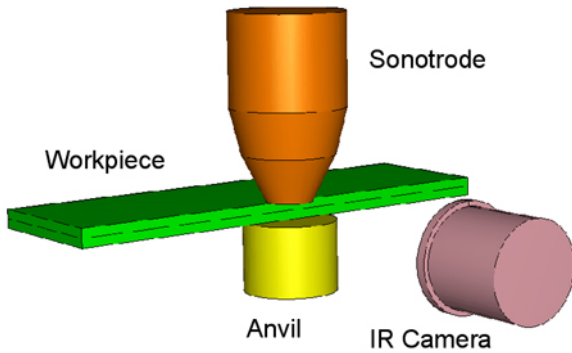


Figure 11. Experimental setup for observing the heat distribution across the weld cross-section.

Figure 12 shows the progression of the heat generation and distribution during welding. The three snap thermal image shots were taken, respectively, at the beginning, middle, and end of the welding cycle. The interfaces and the sonotrode are highlighted to provide the spatial reference frame. It is clear from these images that the heating is predominately generated at the interface and diffused into the workpiece and the sonotrode.

IR thermography was also used to study the formation of cracks caused by the complex acoustic wave distribution in the workpiece. The results are presented in Figure 13. There are two hot spots at the edge of the specimen that were not connected to the main hot spot underneath the sonotrode. This suggests that high level of acoustic energy is concentrated at these locations and causes noticeable heating and cracking at these hot spots.

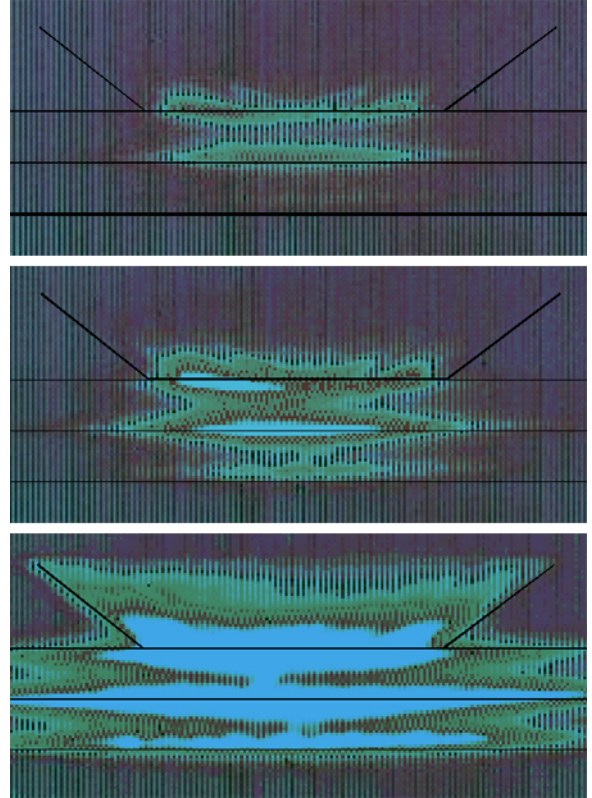


Figure 12. Snapshots of thermal images captured by IR camera at three progressive time instances.

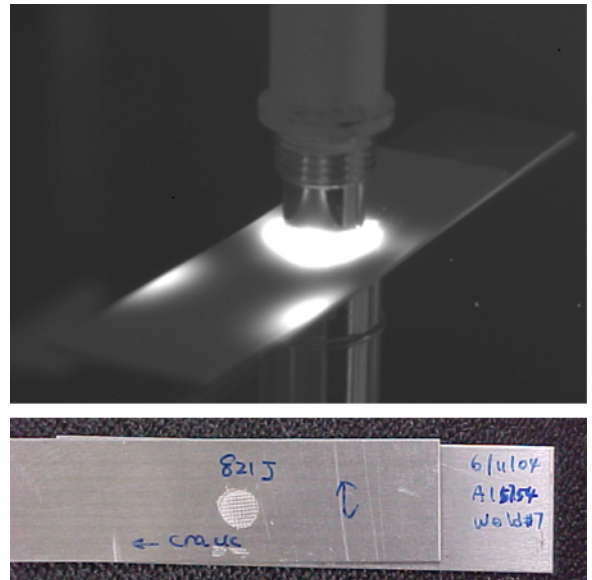


Figure 13. Top: IR thermal image of the “hot” spot. Bottom: the corresponding cracked weld sample.

Figure 14 presents a thermal image of a three-weld sample when the third weld was being made. The weld arrangement and the welding sequence are the same as for the weld sample shown in Figure 10. The concentration of the acoustic energy at the second weld is clearly observed. On the other hand, there is no noticeable heat generation at the first weld, although the first weld is closer to the source of vibration. Also, edge hot spots are evident near the third weld where cracking had been observed.

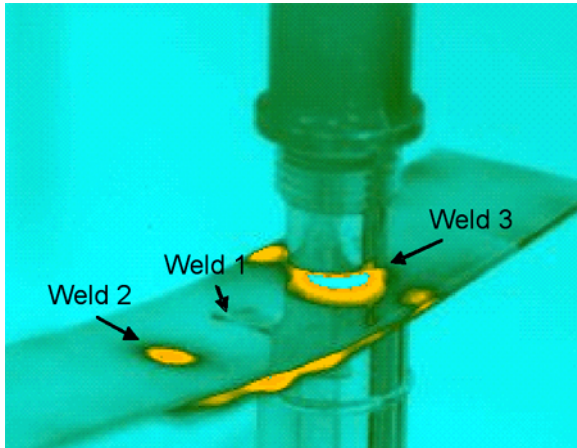


Figure 14. IR Thermal image of multiple spot welds. The third weld is being made.

The initial IR experiment conducted in FY 2004 clearly showed the potential of IR thermography as a tool to study the fundamentals of the UW process. More detailed IR experiments are planned in FY 2005.

Residual Stress Measurement

As in the case of many other welding processes, residual stresses are expected in an ultrasonic weld. High residual stress levels in the bonded region could affect the long-term stability of weld properties in aluminum welds.

Because the bonded region in a spot weld is located between two thin workpieces, measurement of the residual stress in the bonded region is difficult for many measurement techniques such as X-ray diffraction and neutron diffraction.

In this study, the interferometric strain/slope rosette (ISSR) measurement technique, developed by Li and colleagues of Oakland University, was used as an exploratory attempt to investigate the residual stress in a UW weld. The unique features of the

ISSR technique include relatively small gauge size, high precision, and the ability to determine the stress gradient through the workpiece thickness.

The measurement was taken at the center region of the spot weld of Al6061-T6 alloy. The residual stress distributions as a function of the depth from the back side of the weld sample are plotted in Figure 15. σ_{xx} and σ_{yy} are the two normal stress

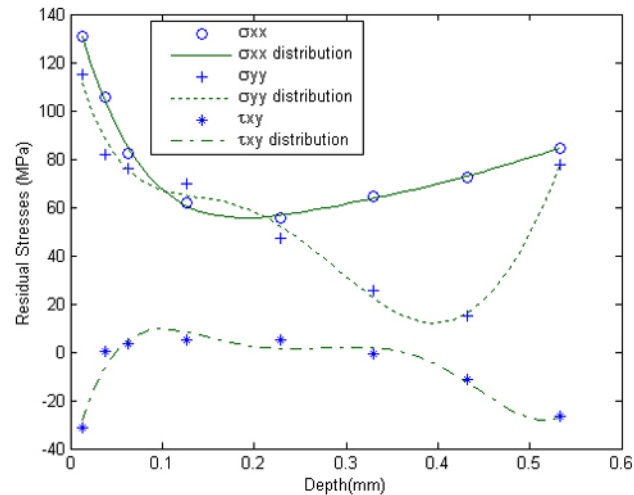


Figure 15. Residual stress as a function of the depth from the back side of an Al6061-T6 weld sample.

components along the length and width of the specimen, respectively, and τ_{xy} is the shear stress component.

The ISSR measurement shows that there are considerable tensile residual stresses in the center region of the ultrasonic weld. The maximum is at the surface of the specimen and reached the yield strength of the material (Table 1). Additional residual stress measurements are planned in FY 2005 to study the effect of welding process conditions on the residual stress.

Conclusions

The research efforts during FY 2004 have resulted in considerable progress toward the understanding of UW process fundamentals. The bonding interface study on dissimilar aluminum alloy welds revealed several important aspects of the interface deformation and bonding process. The profound geometric effects on the acoustic energy propagation and dissipation and the resultant weld properties were identified and characterized.

Publications

W. Ren, K. Li, and Z. Feng, "Ultrasonic Welding Stress Distribution Measured with Optical Rosette/Ring-Core Method," *SAE 2005 Congress*, SAE-International, Technical Paper No 2005-01-1035, 2005.

